University
of Glasgow

http://eprints.gla.ac.uk/94431/

Deposited on: 13 June 2014

Resistive switching in ZrO$_2$ films: physical mechanism for filament formation and dissolution

Pedro Parreira, Stephen McVitie and DA MacLaren

SUPA, School of Physics & Astronomy, University of Glasgow, G12 8QQ Glasgow

Email: p.raimundo-parreira.1@research.gla.ac.uk

Abstract. Resistive switching devices, also called memristors, have attracted much attention due to their potential memory, logic and even neuromorphic applications. Multiple physical mechanisms underpin the non-volatile switching process and are ultimately believed to give rise to the formation and dissolution of a discrete conductive filament within the active layer. However, a detailed nanoscopic analysis that fully explains all the contributory events remains to be presented. Here, we present aspects of the switching events that are correlated back to tunable details of the device fabrication process. Transmission electron microscopy and atomically resolved electron energy loss spectroscopy (EELS) studies of electrically stressed devices will then be presented, with a view to understanding the driving forces behind filament formation and dissolution.

1. Introduction

The need for enormous data density and non-volatile storage has been the motivation behind the development of new memory materials and design concepts [1]. Several competing technologies have been developed in the pursuit of a good candidate that matches the density of Si-based Flash but with increased performance, scalability and power requirements [2]. In recent years, resistive switching random access memory (ReRAM) devices have been extensively studied due to the fact that ReRAM possesses all the properties required for computing and/or data storage, including scalability, non-volatility and rapid switching times [3, 4]. Although much work has been done with resistive switching systems in general, a complete model that describes all known switching phenomena is still lacking and in many ways, recent progress has outpaced a detailed understanding [5]. This is particularly true for the case of memristors based on tantalum and hafnium oxides, which are now commercially available despite the fact that the underlying physics of resistive switching is still under debate [6-8]. It is known that ReRAM relies on electrically induced ion migration in the metal-oxide layers of TaO$_x$, TiO$_x$, ZrO$_x$ and HfO$_x$ systems [1-4]. In these systems a conductive filament (CF) is formed (after an initial electroforming step) by local chemical reduction of an insulating oxide layer located between two contacts [1]. It is the formation of this CF that dramatically lowers the device's resistance between the two electrodes. The application of an electric field with the opposite bias will suppress the CF due to its re-oxidation and restore the high resistance condition (often mediated by local Joule heating) [1-3].

Reproducible resistive switching (RS) is then obtained be repeated CF formation and dissolution, which has recently been observed by *in-situ* TEM measurements [9, 10]. It is accepted that the active electrode plays an important role in this reproducible RS process by acting as a source/sink of oxygen ions [1-5]. A major difference between basic ReRAM devices and these studied here was the introduction of a redox-active insertion layer in the middle of the active layer, which was included to promote the reproducible reduction of the active medium and hence facilitate CF formation [11, 12].

A detailed nanoscopic analysis that fully explains all the contributory events will be essential if issues of device scalability and failure are to be addressed. Given the redox mechanism proposed for CF formation and dissolution, electron transmission microscopy (TEM) and nano-resolved electron energy loss spectroscopy (EELS) are essential tools for unravelling all the mechanisms involved in resistive switching. In this work we present preliminary results of electrically stressed zirconium oxide (ZrO_2) based memristors deposited via pulsed laser deposition (PLD) in an effort to shed some light on some of the resistive switching phenomena.

2. Experimental

Pulsed laser deposition was used to deposit the zirconium oxide active layer using a chamber with a base pressure of 8×10^{-7} Pa and equipped with a load lock and a dry pumping system. The zirconia layer was obtained by ablating a ZrO_2 target with a pulsed 248 nm laser (KrF excimer) with a repetition rate of 18 Hz, a fluence of 3.0 J/cm^2 and an oxygen partial pressure of 0.5 Pa. The deposition temperature was set to 500 ºC during deposition to crystallise the zirconia and activate the Ti insertion layer, substrates were held 8 cm away from the target and were rotating to ensure uniform film coverage. All the devices in this work make use of crossbar architecture with a bottom inert electrode (IE) and a top electrochemically active electrode (AE). The bottom inert electrodes, 90 nm thick, are made from platinum and were deposited using an e-beam thermal evaporation system whereas the active electrodes, also 90 nm thick, are made from titanium and were deposited using a sputtering system. The oxide layer includes a thin titanium insertion layer also deposited by sputtering. Electrical characterisation was made using a LabView controlled Keithley 2602 sourcemeter connected to a temperature controlled probe station. The TEM sample was prepared using a FEI NovaNanolab 200 where a focused ion beam (FIB) was used to isolate a cross section of a memristor and mill it to the required thickness. TEM was performed using a probe corrected JEOL ARM200 CFEG system operating at 200 kV while EELS was done in scanning mode with a Gatan Quantum 965 spectrometer.

3. Results and Discussion

Figure 1 illustrates typical electrical characterisation, which comprises (a) voltage sweeps and (b) endurance cycles where the voltage is pulsed to induce resistive switching. Devices without the Ti insertion layer showed bipolar resistive switching (BRS) but with significantly lower on/off ratios and endurance (Fig. 1, dark curve). These devices also required the current limit enforced by the sourcemeter so that several switching cycles could be performed. The introduction of the Ti insertion layer increases the voltage required for switching but greatly enhances both the on/off ratio and the endurance and reproducibility significantly (Fig.1, light curve). Fig. 2a shows a dark field scanning TEM (STEM) image of the complete device stack, moving left to right, from the bottom platinum IE to the titanium AE and platinum capping layer. Fig. 2b shows normalised elemental distribution measured by EELS in the area indicated. It is clear from elemental quantification analysis that the titanium insertion layer is at least partially oxidised after device cycling, indicating oxygen ion migration within the applied electric field. This insertion layer oxidation is likely to enhance the reduced zirconium CF formation and hence explain the enhanced BRS observed. Another interesting observation lies in the fact that the active layer/active electrode interface (which is approximately 15

nm thick) seems to be oxidised as well, since the oxygen signal drops significantly after the Zr signal and within the Ti electrode itself.
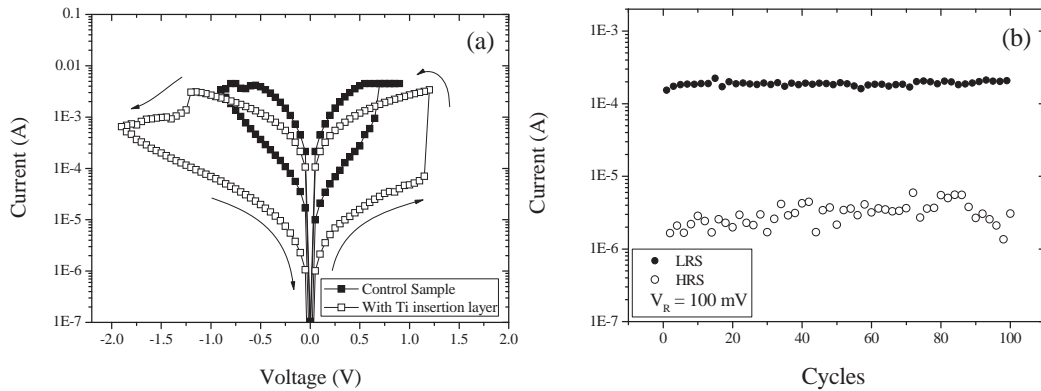
Figure 1 – *(a) iV curve illustrating different switching characteristics for devices with and without a Ti insertion layer, the later shows much better switching. Arrows indicated the sense of voltage sweep. (b) Resistance switching endurance for 100 write/erase cycles for devices with a Ti insertion layer only.*

The preferential oxidation of the titanium AE in comparison with the IE is also coherent with RS model, where switching from a HRS to a LRS is achieved by the formation of a CF and oxygen migration towards the AE. A further interesting and surprising feature is the apparent reduction of the zirconia active layer back to zirconium metal at the interface with the IE, presumably accounting for the oxygen within the Ti insertion layer. This metallic zirconium layer appears to be at least 15 nm thick, although interface roughening effects should be taken into account.
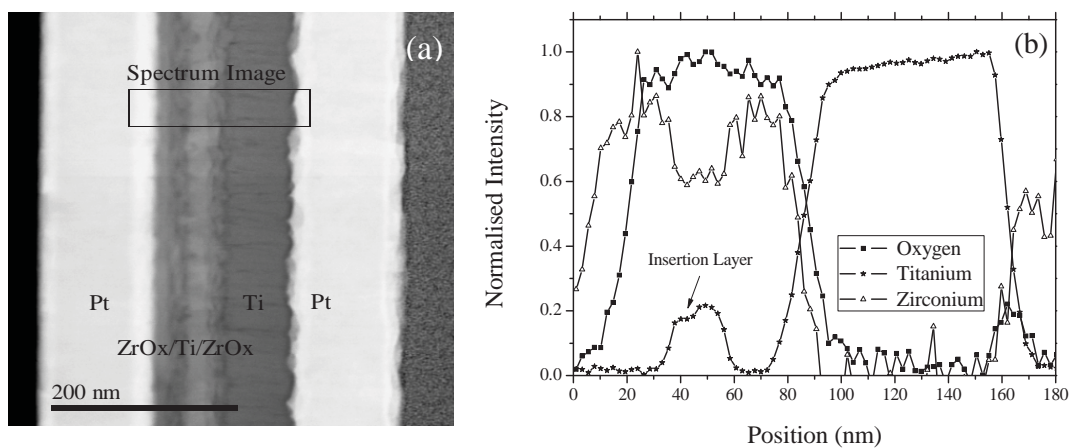
Figure 2 – *(a) Dark field image of a device in cross-section illustrating where EELS analysis was performed and (b) relative elemental quantification. Apparent Zr counts at 160 nm are due to the proximity of the Pt edge whereas the Zr negative counts are attributed to difficulties in background subtraction.*

This implies that it is likely that switching is governed mainly by ionic oxygen movement within the active layer and AE, in agreement with the generally accepted model for CF formation.

4. Conclusions

It was shown that the use of an insertion layer made from an easily oxidisable element enhances the RS performance of memristor devices. This can be explained by the fact that the titanium is oxidised at the expense of zirconia reduction. The localised reduction of the zirconia active layer promotes the conductive filament formation responsible for resistive switching. It was also clear that the use of tools like TEM and EELS is essential if the chemical changes that underpin resistive switching, are to be completely mapped and understood. Future work will focus on more detailed quantification of oxidation states so that in-situ TEM resistive switching can be performed and studied with unprecedented detail.

References

[1]   Balatti, S., Larentis, S., Gilmer, D. C. & Ielmini, D. *Advanced materials* **25,** 1474 (2013).

[2]   Waser, R., Dittmann, R., Staikov, G. & Szot, K. *Advanced Materials* **21,** 2632 (2009).

[3]   Yu, S., Lee, B. & Wong, H. S. P. *Functional Metal Oxide Nanostructures*. **149,** 303 (2012).

[4]   Yang, J. J., Strukov, D. B. & Stewart, D. R. *Nature Nanotechnology* **8,** 13 (2013).

[5]   Lohn, A. J., Stevens, J. E., Mickel, P. R. & Marinella, M. J. *Applied Physics Letters* **103,** 063502 (2013).

[6]   Lee, C. B. *et al. IEEE Electron Device Letters* **32,** 399 (2011).

[7]   Ninomiya, T. *et al.* **48,** 2011 (2012).

[8]   Lee, H. D. *et al. 2012 Symposium on VLSI Technology (VLSIT)* 151–152 (2012).

[9]   Kwon, D.-H. *et al. Nature Nanotechnology* **5,** 148 (2010).

[10]   Yang, Y. *et al. Nature Communications* **3,** 732 (2012).

[11]   Ryu, S. W., Ahn, Y. B., Kim, H. J. & Nishi, Y. *Applied Physics Letters* **100,** 133502 (2012).

[12]   Zhang, H. *et al. Applied Physics Letters* **98,** 042105 (2011).